RSC Advances

ROYAL SOCIETY OF CHEMISTRY

www.rsc.org/advances

Controlling elastico-mechanoluminescence in diphase (Ba,Ca)TiO_3:Pr^{3+} by co-doping different rare earth ions

Jun-Cheng Zhang,[a,e,f,*] Yun-Ze Long,[a,e] Xusheng Wang,[b] and Chao-Nan Xu[c,d,*]

[a]*College of Physics, Qingdao University, Qingdao 266071, P. R. China*

[b]*Functional Materials Research Laboratory, Tongji University, Shanghai 200092, P. R. China*

[c]*National Institute of Advanced Industrial Science and Technology, Kyushu, Shuku 807-1, Tosu, Saga 841-0052, Japan*

[d]*International Institute for Carbon Neutral Energy Research (WPI-I2CNER), Kyushu University, Fukuoka, Japan*

[e]*Key Laboratory of Photonics Materials and Technology in Universities of Shandong, Qingdao University, Qingdao 266071, P. R. China*

[f]*Shanghai Key Laboratory of Special Artificial Microstructure Materials and Technology, Tongji University, Shanghai 200092, P. R. China*

*Corresponding author. E-mail address: jc-zhang@qdu.edu.cn (J. C. Zhang); cn-xu@aist.go.jp (C. N. Xu)

Abstract: Elastico-mechanoluminescence (EML) of diphase (Ba,Ca)TiO_3:Pr^{3+},RE (RE includes all rare-earth-ions except Sc and Pm) is systematically investigated. The EML intensity is obviously controlled by the co-doped RE ions. Y, La, Nd, Gd, Yb, and Lu have the positive effect on improving EML, among which Gd enhances the EML intensity 61% at least. The depth and concentration of traps in (Ba,Ca)TiO_3:Pr^{3+},RE are estimated according to the thermoluminescence curves. The consistent correlation between the dependences of EML intensity and trap concentration on the RE ions illuminates that the change of trap concentration induced by co-doping regulates the EML performance. Furthermore, the similar variations between the EML and afterglow (AG) intensities with the RE ions suggest the possibility that the same types of traps participating in the EML and AG processes. An EML mechanism is proposed on the basis of electrons as the main charge carriers.

Keywords: Elastico-mechanoluminescence; (Ba,Ca)TiO_3:Pr^{3+}; Rare earth ions; Codoping; Thermoluminescence

1. Introduction

Mechanoluminescence (ML) materials, a specific type of solid phosphors, can convert the local mechanical energy into light emission with the application of any mechanical stimulus.[1,2] As a category of ML materials, elastico-mechanoluminescence (EML) materials present an accurate linearity of ML intensity against load in the elastic deformation range, in addition to the mechano-optical conversion.[3,4] The potential of EML materials has been recognized as stress probes to monitor the stress distribution in artificial skin and bone, engineering structures, and living body in view of the advantages such as non-destruction, reproducibility, real-time, and reliability.[5-12] Thus, research for EML materials has continuously gained popularity. More than twenty kinds of inorganic EML materials with different emission spectra from ultraviolet to infrared light have been successfully developed since ZnS:Mn^{2+} and $SrAl_2O_4$:Eu^{2+} were firstly reported in 1999.[5,13] Nevertheless, the number of intense EML materials is quite limited. Among them, $SrAl_2O_4$:Eu^{2+} and ZnS:Mn/Mn,Te/Cu/Cu,Mn have relatively more intense EML.[5,13-17] The brightness can be seen even in day light with naked eyes. Unfortunately, the aluminates and sulfides are chemically unstable, especially very sensitive to moisture, which greatly limits the scope of applications. Accordingly, the water-resistant EML materials, such as silicates $SrCaMgSi_2O_7$:Eu^{2+} and $Ca_2MgSi_2O_7$:Eu^{2+}, aluminosilicates $Ca_2Al_2SiO_7$:Ce^{3+} and $CaAl_2Si_2O_8$:Eu^{2+}, have been synthesized, but their EML intensities are much weaker than that of $SrAl_2O_4$:Eu^{2+}.[18-21] Stable and intense EML materials are thus urgently needed.

Recently, an intense EML has been reported in diphase (Ba,Ca)TiO_3:Pr^{3+}, which is considered one of the promising candidates for the EML applications. The most intense EML brightness achieved at the 60 mol% Ca content is above 15 mcd/m^2, roughly 5000 times the light perception of dark-adapted eye (0.32 mcd/m^2).[22,23] More importantly, the host of this EML material has excellent chemical stability and superior water-resistant behavior.[24] Therefore, to further enhance the EML intensity of diphase (Ba,Ca)TiO_3:Pr^{3+} has very important value to realize the practical application in outdoor and day-light environments.

The interesting multifunctional phenomenon of EML materials provides us a clue to optimize EML performance. The developed EML materials including diphase (Ba,Ca)TiO_3:Pr^{3+} are also long afterglow phosphors (LAPs). As indicated by the previous investigations, both of EML materials and LAPs belong to the defect-controlled type of luminescent materials.[2-14,25] The EML and afterglow (AG) performances are closely related to the trap properties, especially the depth and concentration of trap levels. It is well known that rare earth ions co-doping is an effective concept in regulating the trap properties. It has been presented that the persistent luminescence of LAPs is strongly enhanced by co-doping with selected rare earth ions, e.g. blue LAPs $CaAl_2O_4$:Eu^{2+},Nd^{3+} and $Sr_2MgSi_2O_7$:Eu^{2+},Dy^{3+}, green LAPs $SrAl_2O_4$:Eu^{2+},Dy^{3+} and $CaGa_2S_4$:Eu^{2+},Ho^{3+}, and red LAPs CaS:Eu^{2+},Tm^{3+} and Sr_2SnO_4:Sm^{3+},Dy^{3+}.[26-31] Up to now, countless reports have already been published on the influence of different rare earth ions co-doping on the persistent luminescence of LAPs in order to select the suitable co-doped rare earth ions.[26,29,32] Accordingly, this method has also been used to enhance the EML intensity, but its validity has only been reported in a few cases of $SrAl_2O_4$:Eu^{2+},Dy^{3+}, $Ca_2MgSi_2O_7$:Eu^{2+},Dy^{3+}, and $SrAl_2O_4$:Ce^{3+},Ho^{3+} co-doped by the special rare earth ions.[19,33,34] Even so, less agreement exists on the role of the rare earth codopant. The introduced rare earth ions have been assumed to act as a new trap or to modify the trap properties, such as to deepen the trap depth or to increase trap concentration. The mechanism of EML obtained from the co-doped materials has also not been elucidated. Furthermore, the relation between AG and EML is still unclear. Although most authors agree on the existence of long-lived trap levels related to AG and EML, many details are still shrouded in mystery. In particular, it is wondered that whether the same types of traps are responsible for AG and EML. More importantly, the design and development of new EML materials would be greatly facilitated if the related mechanisms are revealed.

In the present work, different rare earth ions (including Y, La, Ce, Nd, Sm, Eu, Gd, Tb, Dy, Ho, Er, Tm, Yb, and Lu) co-doped diphase (Ba,Ca)TiO_3:Pr^{3+},RE with 60 mol% Ca were synthesized to search for suitable rare earth ions favoring the

enhancement of EML intensity. The new introduced traps, trap depth and trap concentration in these materials were derived from the thermoluminescence (ThL) curves. The role of the rare earth codopant was studied. The nature of traps in $(Ba,Ca)TiO_3:Pr^{3+}$,RE as well as the co-doping effect on the photoluminescence (PL), AG, and EML were discussed in view of the results obtained. The intrinsic relation between AG and EML were assessed according to the similar variation trends among the ThL, AG and EML intensities with the co-doped rare earth ions. Finally, the EML mechanism of $(Ba,Ca)TiO_3:Pr^{3+}$,RE was proposed.

2. Experimental

Diphase $(Ba,Ca)TiO_3:Pr^{3+}$ (BCTP) with the formula $(Ba_{0.4}Ca_{0.6})_{0.998}Pr_{0.002}TiO_3$ and rare earth ions co-doped $(Ba,Ca)TiO_3:Pr^{3+}$,RE (BCTPRE) with the formula $(Ba_{0.4}Ca_{0.6})_{0.996}Pr_{0.002}RE_{0.002}TiO_3$ (RE = Y, La, Ce, Nd, Sm, Eu, Gd, Tb, Dy, Ho, Er, Tm, Yb, and Lu) were synthesized in air by the solid-state reaction method. Raw materials of $BaCO_3$, $CaCO_3$, TiO_2, Pr_6O_{11}, and various trivalent rare earth oxides RE_2O_3 ($\geq$ 99.9%) were mixed thoroughly and prefired at 900°C for 4 h, then remixed, and subsequently sintered at 1400 °C for 4 h. To evaluate the EML property, the synthesized products were ground and screened through a 20 μm sieve, and then mixed in a transparent epoxy resin at a weight ratio of 1:9 (0.5 g : 4.5 g) to form the plastic disks 25 mm in diameter and 15 mm thick.

The structural characterization was examined by X-ray diffraction (XRD, D8 Advance, Bruker AXS Gmbh). Photoluminescence (PL) was recorded with a fluorescence spectrometer (LS-55, Perkin-Elmer). The ThL curves were measured by combining a fluorescence spectrometer (FP-6600, Jasco Co.) with an in-house made temperature control unit. In order to actually compare the PL and ThL curves of different rare earth ions co-doped samples with those of $(Ba,Ca)TiO_3:Pr^{3+}$, the screened $(Ba,Ca)TiO_3:Pr^{3+}$ and $(Ba,Ca)TiO_3:Pr^{3+}$,RE powders with the same weight (0.5 g) were prepared. Compressive stress was applied on the composite disk with a universal testing machine (RTC-1310A, Orientec Corp.). The EML intensity was measured with a computer-driven photon-counting system that consists of a

photomultiplier tube (R649, Hamamatsu Photonics K. K.) and a photon counter (C3866, Hamamatsu Photonics K. K.). Prior to the EML and ThL measurements, all the samples were irradiated at 254 nm for 1 min with a 6 W conventional ultraviolet (UV) lamp, and then the measurements were executed after the delay of 1 min. All measurements except ThL were performed at room temperature. All measurements were executed twice at least, and the experimental results have better repeatability.

3. Results and discussion

3.1 Crystallographic investigation of (Ba,Ca)TiO_3:Pr^{3+},RE

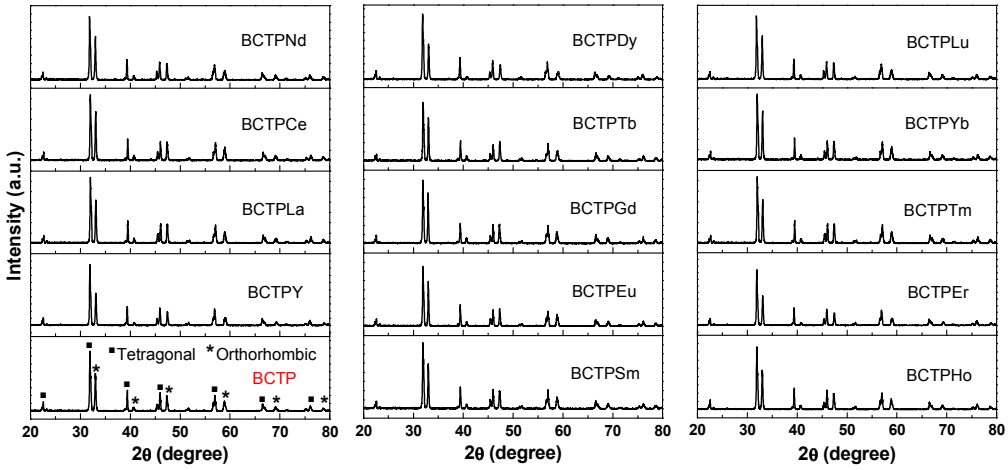

Figure 1. XRD patterns of $(Ba_{0.4}Ca_{0.6})_{0.998}Pr_{0.002}TiO_3$ (BCTP) and $(Ba_{0.4}Ca_{0.6})_{0.996}Pr_{0.002}RE_{0.002}TiO_3$ (BCTPRE, RE = Y, La, Ce, Nd, Sm, Eu, Gd, Tb, Dy, Ho, Er, Tm, Yb, and Lu).

Figure 1 shows the powder XRD patterns of $(Ba_{0.4}Ca_{0.6})_{0.998}Pr_{0.002}TiO_3$ (BCTP) and $(Ba_{0.4}Ca_{0.6})_{0.996}Pr_{0.002}RE_{0.002}TiO_3$ (BCTPRE). BCTP has a diphase coexistence of the tetragonal piezoelectric phase $Ba_{0.77}Ca_{0.23}TiO_3$:Pr^{3+} and the orthorhombic phosphor phase $Ba_{0.1}Ca_{0.9}TiO_3$:Pr^{3+}. The stoichiometries of $Ba_{0.77}Ca_{0.23}TiO_3$:Pr^{3+} and $Ba_{0.1}Ca_{0.9}TiO_3$:Pr^{3+} have been calculated to be 44.8 mol% and 55.2 mol%, respectively. Our previous reports have indicated that EML in diphase (Ba,Ca)TiO_3:Pr^{3+} comes from the interaction of sandwich architectures composed of

piezoelectric phase and phosphor phase.[22,23] The XRD patterns of (Ba,Ca)TiO_3:Pr^{3+},RE do not contain any impure phase in comparison with that of (Ba,Ca)TiO_3:Pr^{3+}, indicating that low concentration of rare earth ions co-doping has no remarkable influence on the crystalline structure.

3.2 Photoluminescence properties of (Ba,Ca)TiO_3:Pr^{3+},RE

Figure 2 shows the PLE (λ_{em} = 613 nm) and PL (λ_{ex} = 343 nm) spectra of BCTP and selected BCTPRE. All of the co-doped rare earth ions cause the decrease of PLE and PL intensities, but none of them were found to affect the locations of PLE and PL peaks, as well as the shape of spectra. The relative PL integral intensities of BCTPRE are plotted and compared in Figure 3. Among them, Ce co-doping has the most serious quenching effect on the emission.

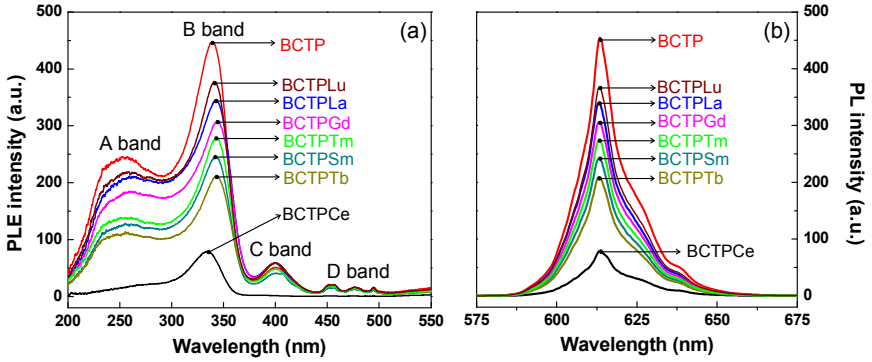

Figure 2. (a) Photoluminescence excitation (PLE, λ_{em} = 613 nm) and (b) photoluminescence (PL, λ_{ex} = 343 nm) spectra of (Ba,Ca)TiO_3:Pr^{3+} (BCTP) and selected (Ba,Ca)TiO_3:Pr^{3+},RE (BCTPRE).

Figure 2a shows that the excitation spectra are composed of four bands: two strong broad bands centered at ~256 nm (A band) and ~343 nm (B band), a weak broad band centered at ~400 nm (C band), as well as the weak peaks (D band) at 456, 476, and 494 nm, respectively. These results are in good agreement with our previous reports on $CaTiO_3$:Pr^{3+} and diphase (Ba,Ca)TiO_3:Pr^{3+}.[35,36] A band is ascribed to the lowest field component of the 4f5d state of Pr^{3+}. B band is assigned to the

valence-to-conduction band transition [O(2p)-Ti(3d)]. C band is attributed to a low-lying Pr-to-metal (Pr^{3+}-Ti^{4+}) intervalence charge transfer state (CTS), by which photo-electrons are radiationlessly de-excited from the $^3P_0$ state to the $^1D_2$ state of Pr^{3+}. The weak peaks (D band) at 456, 476, and 494 nm originate from $^3H_4$ to ^3P_J (J = 0, 1, 2) transitions of Pr^{3+}, respectively. It is apparent that rare earth ions co-doping decreases the absorption of 4f5d state of Pr^{3+} (A band) and host (B band), and no energy transfer from the co-doped rare earth ions to Pr^{3+} takes place.

Figure 2b presents that the main emission peaks of BCTPRE all lie in 613 nm, which are ascribed to the $^1D_2$-$^3H_4$ transition of Pr^{3+}.[35,36] Rare earth ions co-doping does not change the PL peak position and spectral shape. No rare earth ions or intrinsic defect related emission has been observed whether the excitation wavelength is 256, 343, 400, 456, 476 or 494 nm for BCTPRE, indicating that neither direct excitation of co-doped rare earth ions nor energy transfer from Pr^{3+} to co-doped rare earth ions occurs. It is well known that the energy absorbed by phosphors will be released mainly by three ways, i.e. light emission, energy transfer, and nonradiative transition. Therefore, the above results suggest that the co-doped rare earth ions could introduce trap centers to capture the excited charge carriers, delaying the recombination emission in Pr^{3+} and suppressing the PL intensity, or create nonradiative recombination centers to compete with Pr^{3+}, quenching PL, rather than form new luminescence centers or act as sensitizers.

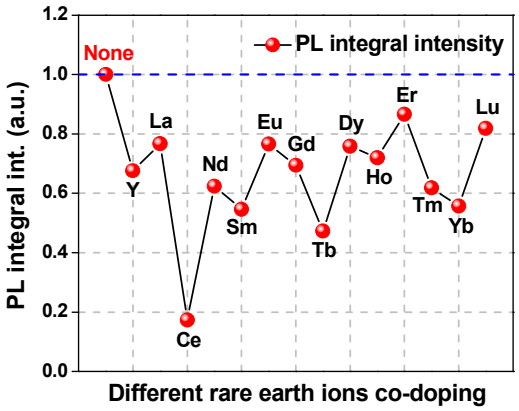

Figure 3. Effect of rare earth ions co-doping on the photoluminescence (PL) integral

intensity of (Ba,Ca)TiO_3:Pr^{3+},RE.

3.3 Elastico-mechanoluminescence properties of (Ba,Ca)TiO_3:Pr^{3+},RE

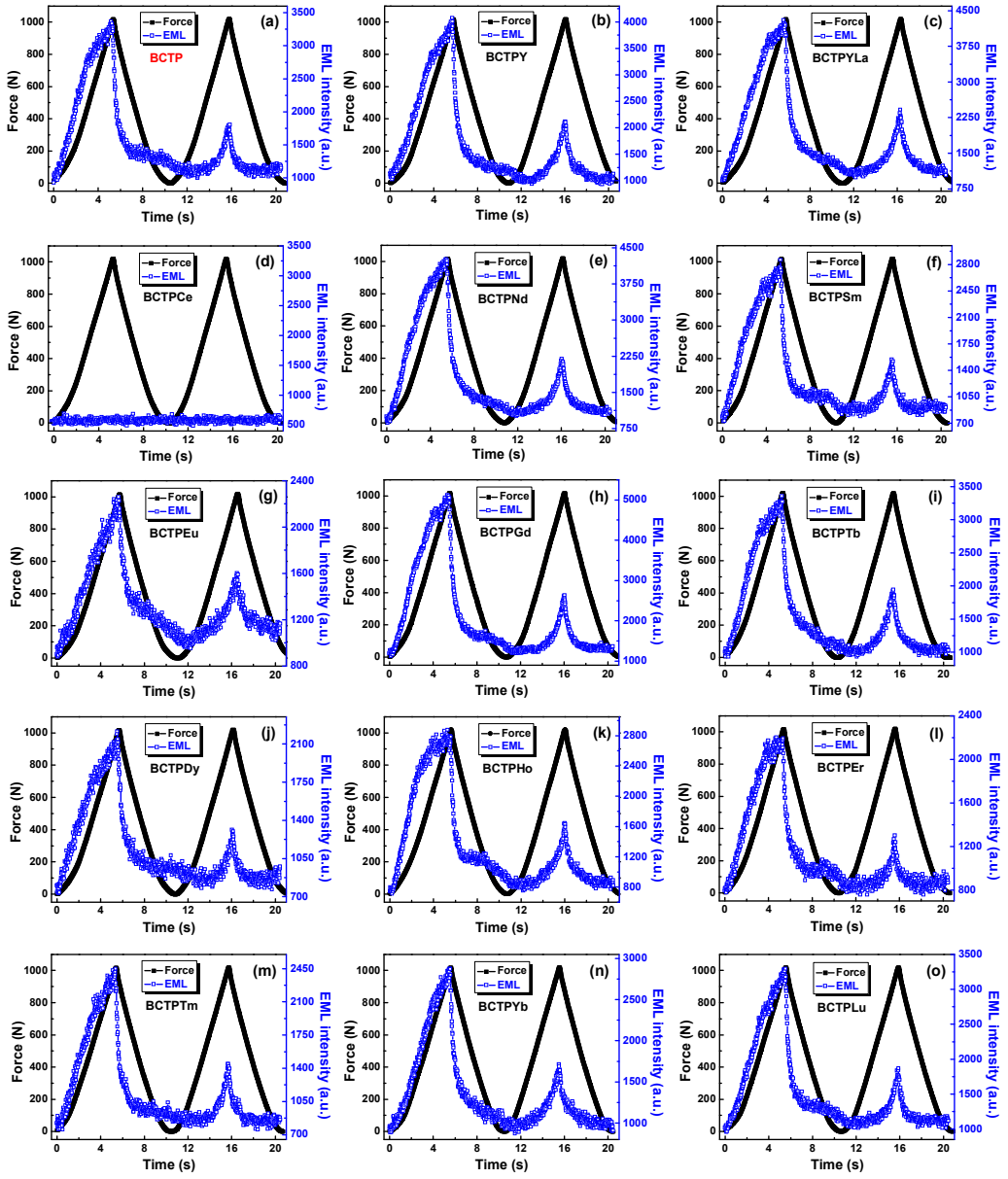

Figure 4. (a) - (o) Elastico-mechanoluminescence (EML) behaviors of (Ba,Ca)TiO_3:Pr^{3+} (BCTP) and (Ba,Ca)TiO_3:Pr^{3+},RE (BCTPRE, RE = Y, La, Ce, Nd, Sm, Eu, Gd, Tb, Dy, Ho, Er, Tm, Yb, and Lu) during the reapplication of compressive triangle load up to 1000 N.

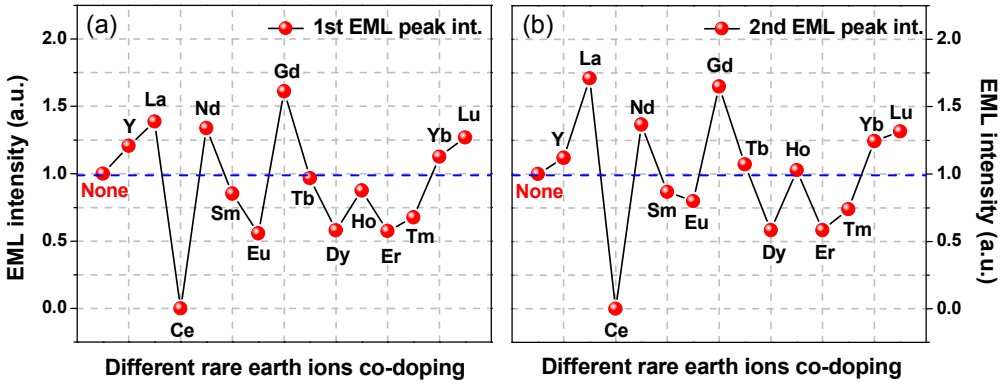

Figure 5. Effect of rare earth ions co-doping on the EML intensity of (Ba,Ca)TiO_3:Pr^{3+},RE: (a) for the 1st EML peak intensity and (b) for the 2nd EML peak intensity.

With a view to investigating the effect of rare earth ions co-doping on the EML performance, the EML behaviors of BCTP and BCTPRE are studied when a repetitive pressure up to 1000 N is applied at a rate of 3 mm/min, as shown in Figure 4. All of the EML curves except that of BCTPCe have a similar EML behavior. In each cycle, the EML intensity linearly changes with the increase of load, showing an EML peak at the peak load. When the load is released, the light is attenuated rapidly. As a repetitive pressure is applied, the EML peak intensity decreases obviously, which is ascribed to the de-trapping process of trapped carriers. It should be noted that the EML intensities of all these samples compressed repetitively will recover completely after the irradiation of UV light (254 nm) for 1 min, indicating the reproducibility of EML. The damage on their samples is very small after the repetitive mechanical experiments, which is useful for the practical application. These results are consistent with those of BCTP.[22-24] However, rare earth ions have apparently different effects on EML. Only a few of rare earth ions (including Y, La, Nd, Gd, Yb, and Lu) enhance the EML intensity, while others have negative effect on EML. Similar with the case of PL, Ce co-doping also has a serious quenching effect on the EML of BCTP, resulting in the total disappearance of EML.

The EML intensities of BCTP and BCTPRE for the 1st EML peak and the 2nd EML peak are compared and shown in Figures 5a and b, respectively. It is evident that the EML intensity depends strongly on the type of co-doped rare earth ions. The co-doping effect on EML intensity has a similar change tendency with rare earth ions for the 1st and 2nd EML peaks. It is worthy of note that, different from the PL results, the EML intensity is improved prominently by several co-doped rare earth ions, including Y, La, Nd, Gd, Yb, and Lu. Among them, Gd and La have the most positive effect. For the 1st EML peak, about 60% enhancement of the EML intensity is obtained by Gd co-doping and about 40% enhancement for La co-doping, while for the 2nd EML peak, about 65% enhancement is obtained by Gd co-doping and about 70% enhancement for La co-doping. On the other hand, Sm, Eu, Dy, Er, and Tm quench EML in varying degrees, in addition to Ce inducing the disappearance of EML. The detailed parameters on the influence of rare earth ions co-doping in the EML intensity are listed in Table S1 (ESI).

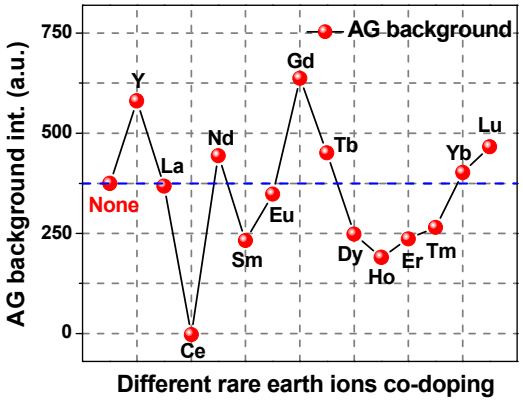

Figure 6. Effect of rare earth ions co-doping on the afterglow (AG) background of $(Ba,Ca)TiO_3:Pr^{3+},RE$.

Furthermore, as indicated in the section of experimental, the EML measurements were executed with the delay of 1 min after the UV irradiation. Thus, the EML intensity at the applied force of 0 N stands for the AG background (i.e. the long afterglow intensity) after stopping the UV irradiation for 1 minute. Figure 6 shows the

effect of rare earth ions co-doping on the AG background of (Ba,Ca)TiO_3:Pr^{3+},RE. Interestingly, there are the similar variations for the EML intensity and AG background with the co-doped rare earth ions. The consistency indicates the EML and AG behaviors are closely related in (Ba,Ca)TiO_3:Pr^{3+},RE, suggesting the possibility that the same types of traps participating in the processes of EML and AG.

3.4 Thermoluminescence analysis of (Ba,Ca)TiO_3:Pr^{3+}

Diphase (Ba,Ca)TiO_3:Pr^{3+} belongs to defect-controlled type of EML materials, and the EML mechanism has been explained by a piezoelectrically induced trapped carrier de-trapping model, in which carriers (electrons or holes) trapped at the trap levels are released under the piezoelectric field induced by mechanical stimulus and then recombine with the luminescence centers, resulting in photon emission.[22-24] Thus, the trap levels play an important role in the EML process. Thermoluminescence (ThL) technique is one of the most effective methods to determine the concentration as well as the depth (i.e. the activation energy) of trap levels in materials. The trap concentration is proportional to the area under the ThL curve. The trap depth E is proportional to corresponding ThL peak temperature. It can be estimated from the slope of the Hoogenstraaten plot and is expressed by the following equation:

$$E = -k \ln(\beta/T_m^2) / (1/T_m) \quad \text{.....(1)}$$

Here, β denotes the constant heating ratio, T_m the maximum peak temperature of the ThL glow curve, and k the Boltzmann constant.[37]

In the present study, the ThL curves of (Ba,Ca)TiO_3:Pr^{3+} were measured from 83.15 K to 483.15 K at different heating rates of 10, 30, 60, and 90 K/min. Before the measurement, UV lighting with a wavelength of 254 nm was irradiated on the sample for 1 min for charging the excitation electrons in the trap levels. The ThL curves are presented in Figure 7. The shape of ThL curve is non-symmetric, suggesting multiple components. Accordingly, the ThL curves were analyzed by Gaussian deconvolution to better investigate the property of trap levels. The fitting result shows that there are two partly overlapping peaks, indicating that at least two kinds of traps exist in BCTP. The Hoogenstraaten plots for different fitting peaks allow us to derive E = 0.096 eV

for Peak 1 and 0.356 eV for Peak 2 (Figure 8). The ThL peaks close to (or above) room temperature are expected to be essential to EML and AG. The location of the Peak 1 is apparently far below room temperature (Figure 7), thus the trap levels corresponding to Peak 1 will be emptied instantaneously at room temperature because of the shallow depth without contribution to the desired EML performance. The trap levels corresponding to Peak 2 with suitable depths could not be thermally activated at room temperature. They are responsible for the reproducible EML and AG phenomenon, but the traps related to EML are emptied faster than in the case of AG due to the application of mechanical stimulation.

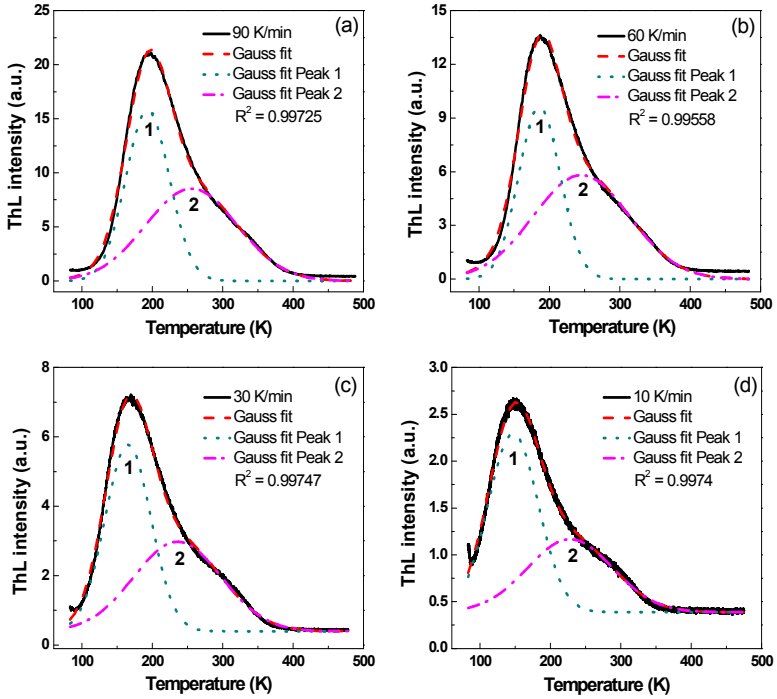

Figure 7. Thermoluminescence (ThL) curves of (Ba,Ca)TiO_3:Pr^{3+} at different heating rate: (a) 90 K/min; (b) 60 K/min; (c) 30 K/min; (d) 10 K/min. Dashed lines are the Gaussian components of ThL glow curves.

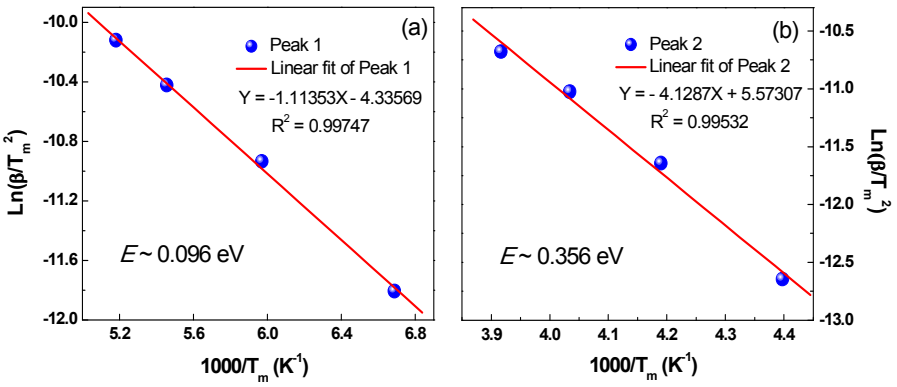

Figure 8. Hoogenstraaten plots for the different ThL peaks of (Ba,Ca)TiO_3:Pr^{3+}: (a) Peak 1; (b) Peak 2.

3.5 Thermoluminescence analysis of (Ba,Ca)TiO_3:Pr^{3+},RE

In order to investigate the co-doping effect on the properties of trap levels, the ThL measurements of (Ba,Ca)TiO_3:Pr^{3+},RE (BCTPRE, RE = Y, La, Ce, Nd, Sm, Eu, Gd, Tb, Dy, Ho, Er, Tm, Yb, and Lu) were also carried out under the same measurement conditions as that of (Ba,Ca)TiO_3:Pr^{3+} (BCTP). Figure 9 presents the ThL curves of BCTPRE at a heating rate of 90 K/min. The ThL curves are fitted using Gaussian deconvolution and the dashed lines are the Gaussian components. The ThL curves of BCTPRE except those of BCTPCe and BCTPEr are composed of three Gaussian peaks (Peak 1, Peak 2, and Peak 3), indicating that at least three kinds of traps exist in BCTPRE. Comparing these ThL Gaussian peaks of BCTPRE with those of BCTP (Figure 7a), in addition to two ThL peaks (Peak 1 and Peak 2) whose location and shape are almost the same as those of BCTP, there is a new low-temperature peak (Peak 3) located at about 160 K for BCTPRE. These results illuminate that rare earth ions co-doping indeed introduces a new kind of trap levels into the phosphors. However, the location of Peak 3 is far below room temperature, thus these trap levels will be emptied at or above room temperature, i.e. without contribution to EML. The same explanation applies to Peak 1. It should be pointed out that for BCTPCe, only the addition of Ce completely suppresses the ThL Peak 2, inducing the disappearance of EML (Figure 4d). This phenomenon also confirms that

Peak 2 in the ThL curve is responsible for the EML process. For BCTPEr, Er co-doping has no effect on introducing new ThL peak. There are still two ThL peaks (Peak 1 and Peak 2), which is similar with BCTP.

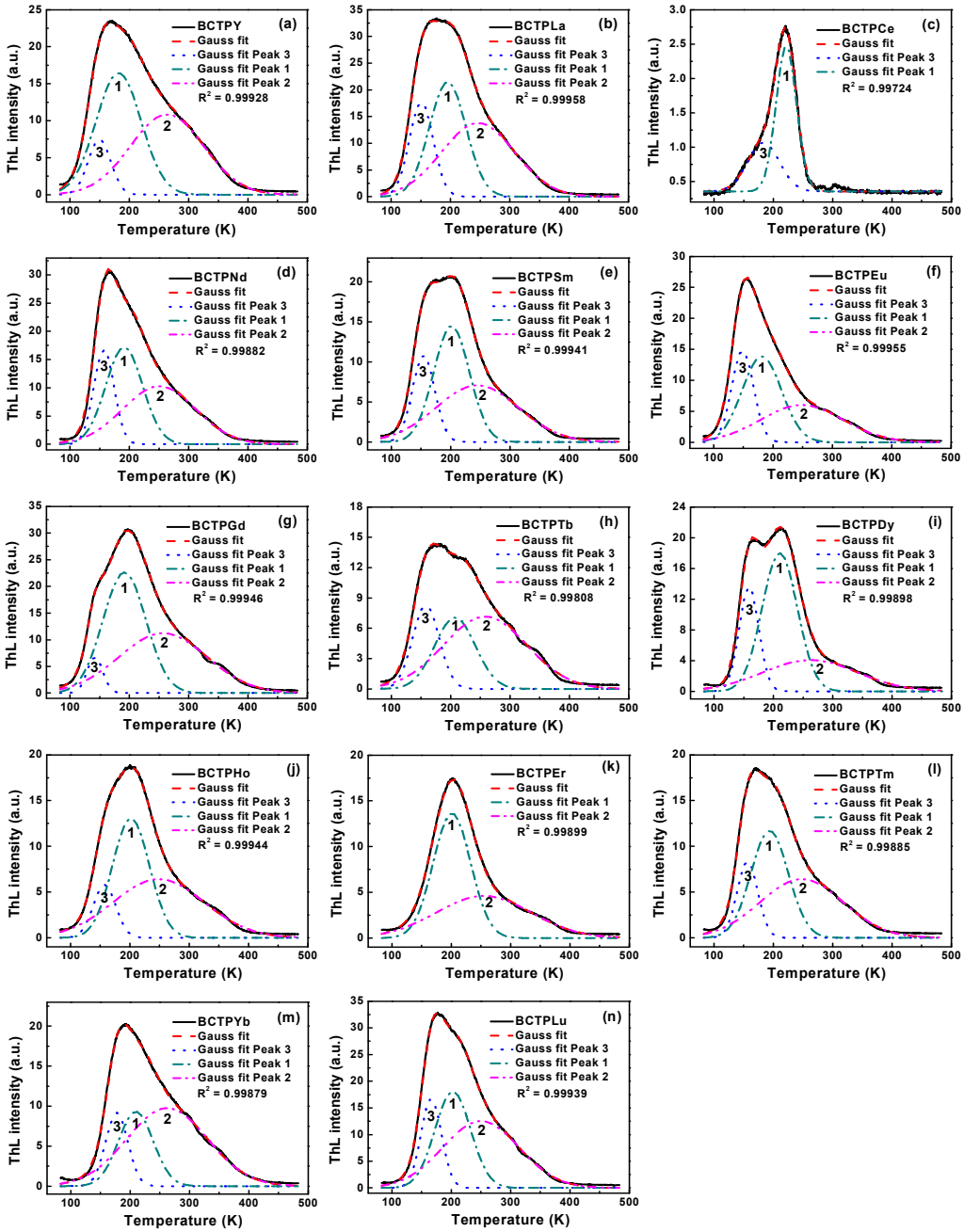

Figure 9. (a) - (n) Thermoluminescence (ThL) curves of (Ba,Ca)TiO_3:Pr^{3+},RE (BCTPRE, RE = Y, La, Ce, Nd, Sm, Eu, Gd, Tb, Dy, Ho, Er, Tm, Yb, and Lu) at a heating rate of 90 K/min. Dashed lines are the Gaussian components of ThL glow

curves.

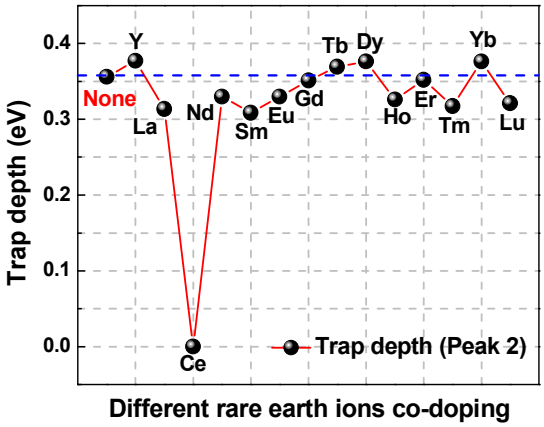

Figure 10. Effect of rare earth ions co-doping on the trap depth (Peak 2) of $(Ba,Ca)TiO_3:Pr^{3+},RE$.

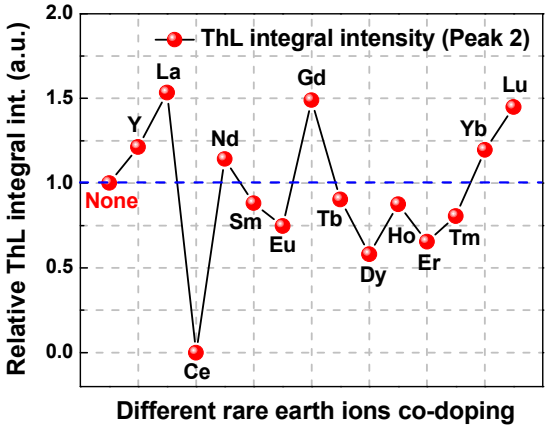

Figure 11. Effect of rare earth ions co-doping on the relative ThL intergral intensity (Peak 2) of $(Ba,Ca)TiO_3:Pr^{3+},RE$.

Considering the dominant role of Peak 2 in the EML process of BCTPRE, the depth of trap levels corresponding to Peak 2 was estimated according to the above-mentioned Hoogenstraaten method. The effect of rare earth ions co-doping on the trap depth and relative ThL intergral intensity corresponding to Peak 2 of $(Ba,Ca)TiO_3:Pr^{3+},RE$ are plotted in Figures 10 and 11, respectively. Table S2 (ESI)

presents these calculated trap depths and ThL intergral intensities of BCTPRE. Obviously, the trap depth seems to be less affected by rare earth ions (except Ce) co-doping. The trap depths of BCTPRE (except BCTPCe) are in the range of 0.30 to 0.38 eV, which are close to that of BCTP (0.356 eV). No correlation was found between the variation trends of trap depth and EML intensity with co-doped rare earth ion when comparing Figure 10 and Figure 6. In contrast, the ThL intensity is strongly influenced by co-doping. The ThL intensity is enhanced by the Y, La, Nd, Gd, Yb, and Lu co-dopings. As noted above, these rare earth ions co-dopings have the same positive effect on the improvement of EML intensity. More importantly, it is apparently observed that the variation of the ThL intensity with co-doped rare earth ion (Figure 11) agrees well with that of the EML intensity (Figure 6). Therefore, it is concluded that the change of trap concentration induced by rare earth ions co-doping has a more significant impact on regulating the EML performance of BCTPRe than that of trap depth. A similar direct correlation has also been found between the long afterglow luminescence and ThL intensity in $CaAl_2O_4:Eu^{2+},RE^{3+}$.[26]

3.6 Elastico-mechanoluminescence mechanism of $(Ba,Ca)TiO_3:Pr^{3+},RE$

It is well known that Pr^{3+} can be oxidized to Pr^{4+} when sintered in air, while Ti^{4+} would get the electron released by Pr^{3+} and be reduced to Ti^{3+}, i.e. Pr^{3+}-e→Pr^{4+} and Ti^{4+}+e→Ti^{3+}, or Pr^{3+}+Ti^{4+}→Pr^{4+}+Ti^{3+}. Thus, several kinds of defects were formed during the synthesis process of $(Ba,Ca)TiO_3:Pr^{3+}$, including calcium and/or barium vacancies ($[V_{Ca/Ba}]''$) to compensate $[Pr_{Ca/Ba}]^o$, Pr^{4+} ($[Pr_{Ca/Ba}]^{oo}$) which tends to form by oxidization of Pr^{3+} after thermal treatment in air, and negatively charged centers like Ti^{3+} ($[Ti_{Ti}]'$) and/or interstitial oxygen $[O_i]''$ correlated with the presence of Pr^{4+}.[38-40] However, except $[Pr_{Ca/Ba}]^o$ as the electron trapping center which participates in the processes of AG and EML, the other defects which are not anticipated from the nominal chemical formulae act as nonradiative recombination centers.[23,35]

In this study, $(Ba,Ca)TiO_3:Pr^{3+},RE$ were synthesized using various trivalent rare-earth oxides RE_2O_3 for the raw materials at high temperature (1400 ^oC) in air. A few of rare earth ions can be easily oxidized into tetravalent state or coexistence of

different valence states, including Ce-Ce^{4+}, Tb-Tb^{3+}/Tb^{4+}, and Dy-Dy^{3+}/Dy^{4+}, while other rare earth ions are mostly trivalent, i.e. Y^{3+}, La^{3+}, Nd^{3+}, Sm^{3+}, Eu^{3+}, Gd^{3+}, Ho^{3+}, Er^{3+}, Tm^{3+}, Yb^{3+}, and Lu^{3+}.[41] It is considered that RE^{3+} and RE^{4+} are incorporated into Ca^{2+} or Ba^{2+} sites according to the acceptable ion radius percentage difference (< 30%) between the doped and substituted ions.[42] Therefore, in the case of (Ba,Ca)TiO_3:Pr^{3+},RE, besides those above-mentioned defects in (Ba,Ca)TiO_3:Pr^{3+}, more point defects arising from the rare earth ions impurity ($[RE_{Ca/Ba}]^{o}$ and $[RE_{Ca/Ba}]^{oo}$) and the Ca or Ba vacancy ($[V_{Ca/Ba}]''$) can be created in the host lattice due to charge compensation. Accordingly, the significant suppress of PL in (Ba,Ca)TiO_3:Pr^{3+},RE (Figures 2 and 3) should be attributed to the formation of more defects hampering the process of energy transfer to Pr^{3+}. It is a typical example that the addition of Ce^{4+} which is known to be a luminescence killer causes a drastic quenching of PL in the several kinds of phosphors.[43-45]

On the other hand, these introduced defects also provide the possibility for regulating the EML properties of (Ba,Ca)TiO_3:Pr^{3+},RE (Figure 5 and Table 1). The results of Figure 11 and Table 2 have indicated that the EML intensity is strongly influenced by the ThL intensity of Peak 2. In (Ba,Ca)TiO_3:Pr^{3+}, the trap corresponding to the ThL Peak 2 has been ascribed to the electron trapping center $[Pr_{Ca/Ba}]^{o}$, which is responsible for the EML process.[21] In (Ba,Ca)TiO_3:Pr^{3+},RE, however, rare earth ions (except Ce) co-doping have less influence on the trap depth corresponding to ThL Peak 2. Therefore, rare earth ions co-doping acts upon regulating the EML intensity through changing the concentration of electron trapping center related to $[Pr_{Ca/Ba}]^{o}$, i.e. $[RE_{Ca/Ba}]^{o}$ introduced by co-doping. It should be noted that the co-doped Ce mainly forms the $[Ce_{Ca/Ba}]^{oo}$ defect in (Ba,Ca)TiO_3:Pr^{3+},Ce prepared in air because of its low reduction potential. The total quenching of EML in Ce do-doped sample suggests the rare earth ions with low reduction potentials (i.e. easily be oxidized to tetravalent state), such as Ce and Dy, present the negative effect on EML (Figure 5 and Table 1). The ability of the rare earth ions to trap electron is probably based on the different reduction potentials. This conclusion can also be confirmed by the result that the most stable rare earth ions (e.g. La, Gd, Lu) with high reduction potentials have the most

positive effect on EML (Figure 5 and Table 1). Nevertheless, the less effect of Tb co-doping on EML possibly arises from the instability of Tb^{4+} in (Ba,Ca)TiO_3:Pr^{3+},Tb.

However, it is still uncertain why different RE^{3+} ions do not have the similar behavior on regulating EML. Because of their rather similar chemical properties, the effect of the RE^{3+} ions should be similar and thus the physical properties, mainly the ionization potentials and the 4f and 5d energy levels may play an important role. The effect of the differences in ionic size and bonding characteristics as well as some redox properties also cannot be excluded. Nevertheless, no correlation was found between the trap depths and the RE^{3+} level locations in this study. The effect of the RE^{3+} co-doping seems to be composed of several factors. The small differences in different factors will finally lead to the large differences observed in the efficiency of EML. Further studies are needed.

Fortunately, it is clear that the increase of EML from the Y, La, Nd, Gd, Yb, and Lu co-doped samples should be attributed to the new introduced electron trapping centers $[RE_{Ca/Ba}]^o$ which have the similar trap depths with $[Pr_{Ca/Ba}]^o$ participating in the EML process. On the other hand, according to the PL, AG and EML results, the $[RE_{Ca/Ba}]^o$ defects formed by the other RE^{3+} ions co-doping possibly act as the nonradiative recombination centers which are adjacent to $[Pr_{Ca/Ba}]^o$ to compete with $[Pr_{Ca/Ba}]^o$, resulting in the EML decrease. The detailed discussion is out of the scope of this work and will be presented elsewhere.

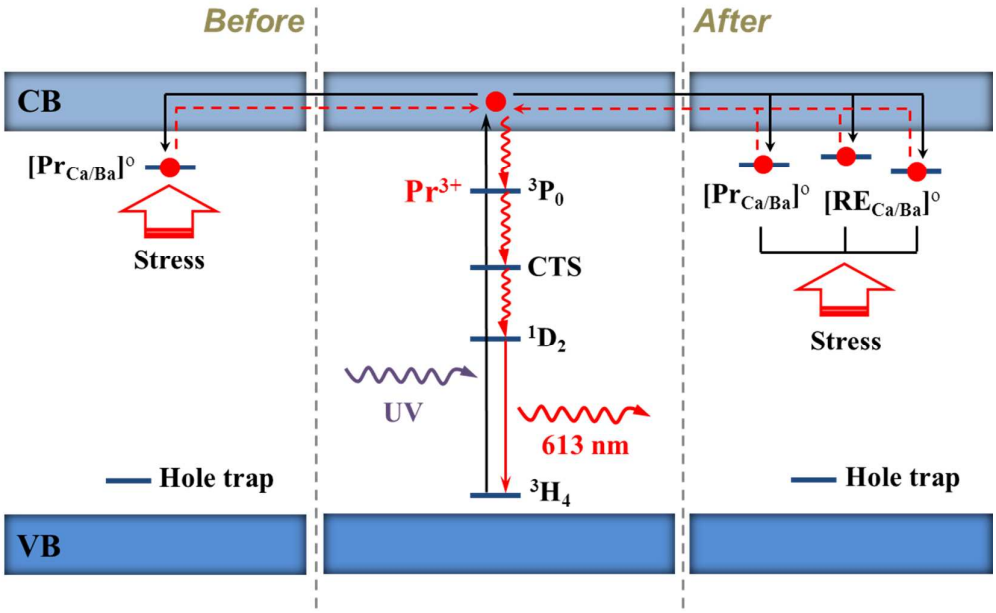

Figure 12. Proposed elastico-mechanoluminescence mechanism before and after co-doping, showing the possible trapping and de-trapping processes of electrons. CTS: charge transfer state.

According to the results previously reported and obtained in this work,[22-24,35,36] the EML processes of (Ba,Ca)TiO_3:Pr^{3+} (before co-doping) and (Ba,Ca)TiO_3:Pr^{3+},RE (after co-doping) are explained based on electrons as the main charge carriers as follows. Figure 12 shows the schematic diagram of EML processes before and after co-doping.

(1) Before co-doping. When (Ba,Ca)TiO_3:Pr^{3+} is irradiated with UV light (254 nm), the electrons are firstly excited from the $^{3}H_4$ ground level of Pr^{3+} to the conduction band of phosphor phase $Ba_{0.1}Ca_{0.9}TiO_3$:Pr^{3+}. Pr^{3+} stays now as Pr^{3+}-h^{+} ionic complex. Then the electrons are trapped by the electron traps ([$Pr_{Ca/Ba}$]^{o}). When the stress is applied, the local piezoelectric field induced by piezoelectric phase $Ba_{0.77}Ca_{0.23}TiO_3$:Pr^{3+} acts on the phosphor phase and leads to the de-trapping of trapped electrons to conduction band. Subsequently, these electrons radiationlessly de-excite from CTS via the $^{3}P_0$ state to the $^{1}D_2$ level of Pr^{3+}-h^{+}. Finally, the relaxation of the electrons back to the ground level of Pr^{3+} emits a red light of 613 nm.

(2) After co-doping. More electron trapping centers [$RE_{Ca/Ba}$]^{o} (RE = Y, La, Nd,

Gd, Yb, Lu) are formed in the host. These traps have the similar depth with $[Pr_{Ca/Ba}]^{o}$. When the electrons of Pr^{3+} are excited to the conduction band, these electrons could be trapped by $[Pr_{Ca/Ba}]^{o}$ and $[RE_{Ca/Ba}]^{o}$ which is adjacent to $[Pr_{Ca/Ba}]^{o}$. Under the application of stress, in contrast to the case before co-doping, more trapped electrons are released from the traps of $[Pr_{Ca/Ba}]^{o}$ and $[RE_{Ca/Ba}]^{o}$ and then come back to luminescent center Pr^{3+}, resulting in more intense EML. Alternatively, other positively charged defects including $[RE_{Ca/Ba}]^{o}$ and $[RE_{Ca/Ba}]^{oo}$ (RE = Ce, Sm, Eu, Dy, Er, Tm) might be created as nonradiative recombination centers after co-doping, hampering the EML process. This process is not depicted in Figure 12.

It is important to note that Pr^{3+} has stronger natural tendency to be oxidized to Pr^{4+} than to be reduced to Pr^{2+}, especially in (Ba,Ca)TiO_3:Pr^{3+} sintered in air. In this work, therefore, electrons are the main charge carriers in the EML mechanism.

4. Conclusions

EML in diphase (Ba,Ca)TiO_3:Pr^{3+} co-doped by various rare earth ions was systematically investigated. The EML intensities of (Ba,Ca)TiO_3:Pr^{3+},RE are controlled by the co-doped RE ions. The Gd co-doping has the most positive effect on EML and the EML intensity is enhanced 61% at least. The similar variations were found between the EML and AG intensities with the RE ions, suggesting the possibility that the same types of traps responsible for EML and AG. The ThL curve of (Ba,Ca)TiO_3:Pr^{3+},RE was used as a reference to study the effect of the rare earth ions co-doping on the properties of traps. A direct correlation between the EML intensity and high-temperature ThL peak intensity was found. The trap depths were affected by co-doping but not as much as the ThL intensity. The results indicate that the change of trap concentration induced by co-doping regulates the EML performance of (Ba,Ca)TiO_3:Pr^{3+},RE. Finally, the EML mechanism of (Ba,Ca)TiO_3:Pr^{3+},RE are explained based on electrons as the main charge carriers.

Acknowledgement

This work was supported by the National Natural Science Foundation of China

(51072136 and 51373082), the Shandong Provincial Natural Science Foundation, China (ZR2013EMQ003), the Program of Science and Technology in Qingdao City (13-1-4-195-jch), the Opening Project of Shanghai Key Laboratory of Special Artificial Microstructure Materials and Technology (ammt2013A-2), the Natural Science Foundation of Shandong Province for Distinguished Young Scholars (JQ201103), the Taishan Scholars Program of Shandong Province (ts20120528), the Program for Scientific Research Innovation Team in Colleges and Universities of Shandong Province, and Grant-in-Aid for Scientific Research (A) (25249100) from JSPS.

References

(1) Walton, J. Triboluminescence. *Adv. Phys.* **1977**, 26(6), 887-948.

(2) Chandra, B. P. Mechanoluminescence. In *Luminescence of Solids*; Vij, D. R., Ed.; Plenum Press: New York, 1988.

(3) Chandra, B. P.; Rathore, A. S. Classification of mechanoluminescence. *Cryst. Res. Technol.* **1995**, 30(7), 885-896.

(4) Xu, C. N. Coatings. In *Encyclopedia of Smart Materials*; Schwartz, M., Ed.; Wiley: New York, 2002.

(5) Xu, C. N.; Watanabe, T.; Akiyama, M.; Zheng, X. G. Artificial skin to sense mechanical stress by visible light emission. *Appl. Phys. Lett.* 1999, 74(9), 1236-1238.

(6) Li, C. S.; Xu, C. N.; Zhang, L.; Yamada, H.; Imai, Y. Dynamic visualization of stress distribution on metal by mechanoluminescence images. *J. Visual-Japan* 2008, 11(4), 329-335.

(7) Terasaki, N.; Xu, C. N. Historical-log recording system for crack opening and growth based on mechanoluminescent flexible sensor. *IEEE Sens. J.* **2013**, 13(1), 3999-4004.

(8) Zhan, T. Z.; Xu, C. N.; Fukuda, O.; Yamada, H.; Li, C. S. Direct visualization of ultrasonic power distribution using mechanoluminescent film. *Ultrason. Sonochem.* **2011**, 18(1), 436-439.

(9) Terasaki, N.; Yamada, H.; Xu, C. N. Ultrasonic wave induced

mechanoluminescence and its application for photocatalysis as ubiquitous light source. *Catal. Today* **2013**, 201, 203-208.

(10) Zhang, J. C.; Xu, C. N.; Kamimura, S.; Terasawa, Y.; Yamada, H.; Wang, X. An intense elastico-mechanoluminescence material CaZnOS:Mn^{2+} for sensing and imaging multiple mechanical stresses. *Opt. Express*, **2013**, 21(11), 12976-12986.

(11) Zhang, J. C.; Xu, C. N.; Long, Y. Z. Elastico-mechanoluminescence in $CaZr(PO_4)_2$:Eu^{2+} with multiple trap levels. *Opt. Express* **2013**, 21(11), 13699-13709.

(12) Chandra, V. K; Chandra, B. P. Dynamics of the mechanoluminescence induced by elastic deformation of persistent luminescent crystals. *J. Lumin.* **2012**, 132(3), 858-869.

(13) Xu, C. N.; Watanabe, T.; Akiyama, M.; Zheng, X. G. Direct view of stress distribution in solid by mechanoluminescence. *Appl. Phys. Lett.* **1999**, 74(17), 2414-2416.

(14) Liu, Y; Xu, C. N. Influence of calcining temperature on photoluminescence and triboluminescence of europium-doped strontium aluminate particles prepared by sol-gle process. *J. Phys. Chem. B* **2003**, 107(17), 3991-3995.

(15) Xu, C. N.; Yamada, H.; Wang, X.; Zheng, X. G. Strong elasticoluminescence from monoclinic-structure $SrAl_2O_4$. *Appl. Phys. Lett.* **2004**, 84(16), 3040-3042.

(16) Reddy, D. R; Reddy, B. K. Laser-like mechanoluminescence in ZnMnTe-diluted magnetic semiconductor. *Appl. Phys. Lett.* **2002**, 81(3), 460-462.

(17) Jeong, S. M.; Song, S.; Lee, S. K.; Ha, N. Y. Color manipulation of mechanoluminescence from stress-activated composite films. *Adv. Mater.* **2013**, 25(43), 6194-6200.

(18) Zhang, H.; Yamada, H.; Terasaki, N.; Xu, C. N. Stress-induced mechanoluminescence in $SrCaMgSi_2O_7$:Eu. *Electrochem. Solid-State Lett.* **2007**, 10(10), J129-J131.

(19) Zhang, H.; Yamada, H.; Terasaki, N.; Xu, C. N. Green mechanoluminescence of $Ca_2MgSi_2O_7$:Eu and $Ca_2MgSi_2O_7$:Eu,Dy. *J. Electrochem. Soc.* **2008**, 155(2), J55-J57.

(20) Akiyama, M.; Xu, C. N.; Matsui, H.; Nonaka, K.; Watanabe T. Recovery phenomenon of mechanoluminescence from $Ca_2Al_2SiO_7$:Ce by irradiation with

ultraviolet light. *Appl. Phys. Lett.* **1999**, 75(17), 2548-2550.

(21) Zhang, L.; Yamada, H.; Imai, Y; Xu, C. N. Observation of elasticoluminescence from $CaAl_2Si_2O_8:Eu^{2+}$ and its water resistance behavior. *J. Electrochem. Soc.* **2008**, 155(3), J63-J65.

(22) Wang, X.; Xu, C. N.; Yamada, H.; Nishikubo, K.; Zheng, X. G. Electro-mechano-optical conversions in Pr^{3+}-doped $BaTiO_3$-$CaTiO_3$ ceramics. *Adv. Mater.* **2005**, 17(10), 1254-1258.

(23) Zhang, J. C.; Wang, X.; Yao, X.; Xu, C. N.; Yamada, H. Strong elastico-mechanoluminescence in diphase $(Ba,Ca)TiO_3:Pr^{3+}$ with self-assembled sandwich architectures. *J. Electrochem. Soc.* **2010**, 157(12), G269-G273.

(24) Zhang, J. C.; Tang, M.; Wang, X.; Li, Y.; Yao, X. Elastico-mechanoluminescence properties of Pr^{3+}-doped $BaTiO_3$-$CaTiO_3$ diphase ceramics with water resistance behavior. *Ceram. Int.* **2012**, 38(S1), S581-S584.

(25) Botterman, J.; Eeckhout, K. V. D.; Baere, I. D.; Poelman, D.; Smet, P. F. Mechanoluminescence in $BaSi_2O_2N_2$:Eu. *Acta Mater.* **2012**, 60(15), 5494-5500.

(26) Aitasalo, T.; Hälsö, J.; Jungner, H.; Lastusaari, M.; Niittykoski, J. Thermoluminescence study of persistent luminescence materials: Eu^{2+}- and R^{3+}-doped calcium aluminates, $CaAl_2O_4:Eu^{2+},R^{3+}$. *J. Phys. Chem. B* **2006**, 110(10), 4589-4598.

(27) Liu, B.; Shi, C.; Yin, M.; Dong, L.; Xiao Z. The trap states in the $Sr_2MgSi_2O_7$ and $(Sr,Ca)MgSi_2O_7$ long afterglow phosphor activated by Eu^{2+} and Dy^{3+}. *J. Alloys Compd.* **2005**, 387(1), 65-69.

(28) Korthout, K.; Eeckhout, K. V. D.; Botterman, J.; Nikitenko, S.; Poelman, D.; Smet, P. F. Luminescence and x-ray absorption measurements of persistent $SrAl_2O_4$:Eu,Dy powders: evidence for valence state changes. *Phys. Rev. B* **2011**, 84(8), 085140.

(29) Guo, C.; Tang, Q.; Huang, D.; Zhang, C.; Su, Q. Influence of co-doping different rare earth ions on $CaGa_2S_4:Eu^{2+},RE^{3+}$ (RE = Ln) phosphors. *J. Phys. Chem. Solids* **2007**, 68(2), 217-223.

(30) Jia, D.; Jia, W.; Evans, D. R.; Dennis, W. M.; Liu, H.; Zhu J.; Yen, W. M. Trapping processes in $CaS:Eu^{2+},Tm^{3+}$. *J. Appl. Phys.* **2000**, 88(6), 3402-3407.

(31) Yu, X.; Xu, X.; Qiu, J. Enhanced long persistence of $Sr_2SnO_4:Sm^{3+}$ red phosphor by co-doping with Dy^{3+}. *Mater. Res. Bull.* **2011**, 46(4), 627-629.

(32) Eeckhout, K. V. D.; Smet, P. F.; Poelman, D. Persistent luminescence in rare-earth codoped image. *J. Lumin.* **2009**, 129(10), 1140-1143.

(33) Yun, G. J.; Rahimi, M. R.; Gandomi, A. H.; Lim, G. C.; Choi, J. S. Stress sensing performance using mechanoluminescence of $SrAl_2O_4$:Eu (SAOE) and $SrAl_2O_4$:Eu, Dy (SAOED) under mechanical loadings. *Smart Mater. Struct.* **2013**, 22(5), 055006.

(34) Zhang, H.; Yamada, H.; Terasaki, N.; Xu, C. N. Ultraviolet mechanoluminescence from $SrAl_2O_4$:Ce and $SrAl_2O_4$:Ce,Ho. *Appl. Phys. Lett.* **2007**, 91(8), 081905.

(35) Zhang, J. C.; Wang, X.; Yao, X. Enhancement of luminescence and afterglow in $CaTiO_3:Pr^{3+}$ by B site Zr substitution for Ti. *J. Alloy. Compd.* **2010**, 498(2), 152-156.

(36) Zhang, J. C.; Yang, W.; Wang, X.; Yao, X. Dielectric and luminescence properties of the A- and B-site doped $CaTiO_3:Pr^{3+}$ ceramics. *Ferroelectrics*, **2010**, 401(1), 226-232.

(37) Hoogenstraaten, W. Electron traps in zinc-sulfide phosphors. *Philips Res. Rep.* **1958**, 13(6), 515-693.

(38) Diallo, P. T.; Boutinaud, P.; Mahiou, R.; Cousseins, J. C. Red luminescence in Pr^{3+}-doped calcium titanates. *Phys. Status Solidi A* **1997**,160(1), 255-263.

(39) Boutinaud, P.; Pinel, E.; Mahiou, R. Luminescence and afterglow in $CaTiO_3:Pr^{3+}$ films deposited by spray pyrolysis. *Opt. Mater.* **2008**, 30(7), 1033-1038.

(40) Zhu, A.; Wang, J.; Zhao, D.; Du, Y. Native defects and Pr impurities in orthorhombic $CaTiO_3$ by first-principles calculations. *Physica B* **2011**, 406(13), 2697-2702.

(41) Sroor, F. M. A.; Edelmann, F. T. *Lanthanides: Tetravalent Inorganic*. In The Rare Earth Elements: Fundamentals and Applications,; Atwood, D. A., Ed.; Wiley: New York, 2012.

(42) Shannon, R. D. Revised effective ionic radii and systematic studies of interatomie distances in halides and chaleogenides. *Acta Cryst.* **1976**, A32, 751-767.

(43) Nag, A.; Kutty, T. R. N. Photoluminescence of $Sr_{2-x}Ln_xCeO_{4+x/2}$ (Ln = Eu, Sm or

Yb) prepared by a wet chemical method. *J. Mater. Chem.* **2003**, 13(2), 370-376.

(44) Potdevina, A.; Chadeyrona, G.; Brioisc, V.; Mahioub, R. Structural, morphological and scintillation properties of Ce^{3+}-doped $Y_3Al_5O_{12}$ powders and films elaborated by the sol-gel process. *Mater. Chem. Phys.* **2011**, 130(1-2), 500-506.

(45) Kitsuda, M.; Fujihara, S. Quantitative luminescence switching in $CePO_4$:Tb by redox reactions. *J. Phys. Chem. C* **2011**, 115(17), 8808-8815.